Electronic Supplementary Information (ESI)

Effects of Molecular Weight Fractionated Humic Acid on the Transport and Retention of Quantum dots in Porous Media

Jiangli Yang,[1a] Piao Xu,[1a] Liang Hu,[1b] Guangming Zeng,[*a] Anwei Chen, [*c] Kai He,[a] Zhenzhen Huang,[a] Huan Yi,[a] Lei Qin[a] and Jia Wan[a]

[a] *College of Environmental Science and Engineering, Hunan University, and Key Laboratory of Environmental Biology and Pollution Control (Hunan University), Ministry of Education, Changsha, Hunan 410082, P.R. China.*

[b] *School of Minerals Processing and Bioengineering, Central South University, Changsha, 410083, P.R. China*

[c] *College of Resources and Environment, Hunan Agricultural University, Changsha, Hunan, 410128, PR China.*

[*]Corresponding authors. Address: College of Environmental Science and Engineering, Hunan University, Changsha 410082, P.R. China. Tel.: +86 731 88822829; fax: +86 731 88823701

E-mail addresses: zgming@hnu.edu.cn (G. Zeng), A.Chen@hunau.edu.cn (A. Chen)

[1] These authors contribute equally to this article.

Supplemental Methods:

1. Porous media

The pure quartz sands (40-70 mesh, Sigma-Aldrich, Shanghai, China) were sifted through 40 and 70 mech sieves to obtain a fraction of an average sand diameter of 265 μm,[1] and then the sand was cleaned exhaustively by the process described elsewhere[2, 3] to remove orgonic contaminants and metal impurity. Briefly, the sand was soaked in 70% HNO_3 for at least 16 h and rinsed with deionized (DI) water until the pH was close to neutral. Afterwards, the sand was immersed into 0.5 M NaCl solution for 1 h in sonicate, rinsed with DI water, and then sonicates in DI water for 1 h. These steps (i.e. soaking in NaCl, flushing with water, and sonication) were repeated until the absorbance of supernatant was negligible as confirmed by UV/Vis. After the throughly cleaning treatment, the sand was dried and conducted using scanning electron microscopy (SEM). The SEM (Figure S6) images showed that the surfaces of sand were cleanly and indicated the majority of clay particles removed by this treatment.

The zeta potential of the clean sand in the over range of background solution studied in the transport experiments were assessed by Zetasizer Nano ZS (Malven Instruments, UK) using the method described by Tufenkji and Elimelech.[4] Briefly, 7 g of clean sand was sonicated (Aquasonic 150T, VWR Scientific Products, West Chester, PA) for 20 min in 12 mL of the background solution of interest. Following sonication, samples of the supernatant were diluted 10-fold in the background

electrolyte solution and the zeta potential measurement was using Zetasizer Nano ZS (Malven Instruments, UK). Result of the measurement was shown in Table S6, all the measurements were conducted at least triplicate.

2. HA adsorbed on QDs

A batch of experiments were conducted to quantify the amounts of HA adsorbed onto QDs under various conditions. The procedure of measuring the adsorbed amount of HA was following by the method described by Morales et al.[5] Immediately after the accomplishing of the QDs suspension preparation described in the study, 100 uL of QDs suspension was added into 50-ml centrifuge tubes that contained 20ml QD-free background electrolyte, and stirred 24h for equilibrium. Then, centrifuge at 8000 rpm (ca. 8520 g) for 2h to settle QDs-HA complex. The supernatant was analyzed for HA concentration by measuring the TOC concentration. The effectiveness of the methodology was verified using an inductively coupled plasma-optical emission spectrophotometer (ICP-OES, Perkin Elmer 208 OPTIMA 3300 DV), and the centrifugation step was verified to not significantly influence the concentration of non-adsorbed HA components.[6] The difference between the initial and final concentration of HA is the adsorbed amount of HA. The results were reported as mg HA/m^2 QDs for each condition. It was noted that all samples were produced in duplicate including the control.

3. Estimation of the thickness layer of HA on QDs

Following the method described by Phenrat et al.,[7, 8] the thickness of adsorbed

HA layer on QDs in both NaCl and $CaCl_2$ solutions are obtained. the experimental values of electrophoretic mobility(u_e) (present of HA) and zeta potential ζ (QDs in NaCl or in $CaCl_2$) were fitted the Ohshim's soft particle model to obtain the best fits of N, λ, and d.[8, 9] Briefly, the procedure including fitting the equation (1), together with the terms defined as Eq. (2)-(5) to the experiment data of u_e and ζ under different conditions to derive the thickness of adsorbed HA layer on QDs (d), the softness of the coated particles (λ^{-1}), and the number concentration of the dissociated functional groups in the adsorbed HA layer. A MATLAB (Matlab R2012a, the Mathworks) code employing iterative least squares minimization was used for fitting.

$$u_e = \frac{\varepsilon_0 \varepsilon_r}{\eta} \frac{\psi_0 / \kappa_m + \psi_{DON} / \lambda}{1/\kappa_m + 1/\lambda} f\left(\frac{\mathrm{d}}{a}\right) + \frac{ZeN}{\eta\lambda^2} + \frac{8\varepsilon_0 \varepsilon_r k_B T}{\eta z e \lambda} \tanh\left(\frac{ze\zeta}{4k_B T}\right) \frac{e^{-\lambda d}/\lambda - e^{-\kappa_m d}/\kappa_m}{1/\lambda^2 - 1/\kappa_m{}^2} \tag{1}$$

$$\psi_{DON} = \frac{k_B T}{ze} \ln\left\{\frac{ZN}{2zn^{\infty}} + \left[\left(\frac{ZN}{2zn^{\infty}}\right)^2 + 1\right]^{1/2}\right\} \tag{2}$$

$$\psi_0 = \psi_{DON} - \frac{k_B T}{ze} \tanh\left(\frac{ze\psi_{DON}}{2k_B T}\right) + \frac{4k_B T}{ze} \tanh\left(\frac{ze\zeta}{4k_B T}\right) e^{-\kappa_m d} \tag{3}$$

$$f\left(\frac{\mathrm{d}}{a}\right) = \frac{2}{3}\left[1 + \frac{1}{2(1+d/a)^3}\right] \tag{4}$$

$$\kappa_m = \kappa\left[1 + \left(\frac{ZN}{2zn^{\infty}}\right)^2\right]^{1/4} \tag{5}$$

where ε_0 is the vacuum permittivity; ε_r is the relative permittivity of solution; η is the dynamic viscosity of solution; a is the radius of the core QDs; k_B is the Botlzmann's constant; T is the absolute temperature; e is the elementary electric charge; k^{-1} is the Debye-Hückel length of solution; κ_m is the Debye- Hückel parameter of the adsorbed

HA layer that involves the contribution of the fixed-charges N; ψ_{DON} is the Donnan potential in the HA layer; ψ_0 is the potential at the boundary between the polyelectrolyte layer and the surrounding solution; Z and N are the valence and the number concentration of the dissociated functional groups in the polyelectrolyte layer, respectively; z and n^{∞} are the valence and the bulk number concentration of the electrolyte, respectively.

4. Calculation of interaction energies

4.1 DLVO Interaction Energy Calculations

Derjaguin-Landau-Verwey-Overbeek (DLVO) theory was used to calculate the total interaction between QDs and sand under different solution chemistry conditions. Electrical double layer (EDL) repulsion, van der Waals (VDW) attraction forces were considered in DLVO theory.[10] The particle-collector interaction can be treated as sphere-plate interaction case. The van der Waals attractive interaction (V_{vdw}) for a sphere-plate case was calculated using the approach of Elimelech and Omelia: [11]

$$V_{vdw} = -\frac{A_{123} a_p}{6x}\left(1+14x/\lambda_c\right)^{-1} \tag{6}$$

Where a_p is the particle radius (m); x is the separation distance between nanoparticles and plate surface; λ_c is the characterisic wavelength of interaction, often taken as 100 nm. The V_{edl} for sphere-plate interactions was calculated with the following expression.[11]

$$V_{edl} = \pi\varepsilon\varepsilon_0 a_p \left\{ 2\varphi_1\varphi_2 \ln\left[\frac{1+\exp\left(-kx\right)}{1-\exp\left(-kx\right)}\right] + \left(\varphi_1^{\,2}+\varphi_2^{\,2}\right)\ln\left[1-\exp\left(-2kx\right)\right]\right\}, \tag{7}$$

Where ε_0 is the vacuum permittivity; ε is the relative permittivity of water; k is the

Debye reciprocal length; φ_1 and φ_2 are the surface potential of the QDs nanoparticle and the plate surface, respectively; A_{123} is the Hamaker constant for QDs-water-sand system. The surface potential of QDs and sand can be determined following van Oss et al.[12]:

$$\psi_0 = \xi\left(1 + \frac{x}{a_p}\right)exp(kx), \quad (8)$$

Where x is the distance between the surface and the charged particle and the slipping plane is usually taken as 0.5 nm.

The Hamaker constant for QDs-water-sand system can be calculated from the Hamaker constant of the individual material by following equation. [13]

$$A_{123} = \left(\sqrt{A_{11}} - \sqrt{A_{22}}\right)\left(\sqrt{A_{33}} - \sqrt{A_{22}}\right), \quad (9)$$

Where $\sqrt{A11}$ is the Hamaker constant for QDs nanoparticle. The value of Hamaker constant for QDs in the absence of HA is taken from Radich[14] as 6.13×10^{-20} J. HA would adsorb onto QDs when HA present in the aqueous solutions, thus, the Hamaker constant for HA (4.85×10^{-20}) is employed to present the Hamaker constant for QDs when HA present in the solution.[15, 16] $\sqrt{A22}$ is the Hamaker constant for the medium that particle suspension. In this study, the Hamaker constant for water is taken from Israelachvili[13] as 3.70×10^{-20} J; $\sqrt{A33}$ is the Hameker constant for sand is taken from Israelachvili[13] as 6.50×10^{-20} J. The result from Eq (8) for the Hamaker constant for the QDs-water-sand is 3.46×10^{-21}J in the absence of HA and 1.74×10^{-21}J in the presence of HA, respectively.

3.2 Modified DLVO interaction energy calculations

In order to better understand the effect of pristine- and M_f-HA on the transport

and retention of QDs in different electrolytes. The DLVO interaction energy calculations were modified by the incorporated of a steric repulsion energy when HA coated QDs particles approach to sand. Steric repulsion including osmotic repulsion (Vosm) and elastic-steric repulsion (Velas).[7, 17] Overlap of the polymer layers on two approaching particles increases the local polymer segment concentration and thus increases the local osmotic pressure in the overlap region (V_{osm}). Any compression of the adsorbed polymer layers below the thickness of the unperturbed layer (d) leads to a loss of entropy and gives rise to the elastic pulsion (V_{elas}). V_{osm} can be written as below: [17]

$$\frac{V_{osm}}{K_B T} = 0 \qquad 2d \le x \tag{10}$$

$$\frac{V_{osm}}{K_B T} = \frac{a_p 4\pi}{v_1} \varphi_p^2 \left(\frac{1}{2} - \chi\right)\left(d - \frac{x}{2}\right)^2 \qquad d \le x \le 2d \tag{11}$$

$$\frac{V_{osm}}{K_B T} = \frac{a_p 4\pi}{v_1} \varphi_p^2 \left(\frac{1}{2} - \chi\right) d^2 \left(\frac{d}{2x} - \frac{1}{4} - ln\left(\frac{x}{d}\right)\right) \qquad x < d \tag{12}$$

where χ is the Flory-Huggins solvency parameter, which is assumed to be 0.45 for HA/water interaction; v_1 is the volume of a solvent molecule (0.03 nm^3) φ_p is fractional HA surface coverage; d is the thickness of the adsorbed HA layer.

V_{elas} was calculated with the following equation:[17]

$$\frac{V_{elas}}{K_B T} = 0 \qquad d \le x$$

（13）

$$\frac{V_{elas}}{K_B T} = \frac{a_p \pi}{M_W} \varphi_p d^2 \rho_p \left[\frac{x}{d} ln\left(\frac{x}{d} \left(\frac{3 - \frac{x}{d}}{2} \right)^2 \right) - 6ln\left(\frac{3 - \frac{x}{d}}{2} \right) + 3\left(1 + \frac{x}{d} \right) \right] \qquad d > x$$

（14）

where M_W is the molecular weight of the HA and ρ_p is its density.

The total interaction (V_T) was calculated with the following equation:

$$V_T = V_{vdw} + V_{edl} + V_{osm} + V_{elas}$$

（15）

Supplemental Tables:

Table S1. TOC concentration and carbon weight percent (wt%) of the M_f-HA collected after ultrafiltration separation.

HA type	TOC (mg/L)	Carbon weight percent (%)
Pristine HA	174.5	
>100 kDa HA	1682.25	13.4
30-100 kDa HA	4872.75	33.2
10-30 kDa HA	2974.5	22.3
3-10 kDa HA	419	12.2
< 3 kDa HA	17.72	9.9
Total recovery	/	91.0

Table S2. Zeta potentials, particle size of QD-COOH in the absence and presence of pristine- and M_r-HA in 3 mM NaCl or 2 mM $CaCl_2$ solutions.

	NaCl			**$CaCl_2$**	
HA type	**Zeta potential (mV)**	**DLS diameter (nm)**	**TEM Diameter (nm)**	**Zeta potential (mV)**	**DLS diameter (nm)**
no HA	-31.4±0.7	113 ± 22	32 ± 24	-9.2±0.6	538 ± 18
pristine HA	-33.3±3.2	109 ± 52		-12.7±0.1	226 ± 9
>100 kDa HA	-34.3±0.4a	97 ± 33b	29 ± 22	-11.8±0.0a	235 ± 6a
30-100kDa HA	-32.4±0.0a	114 ± 28b		-12.7±0.1d	185 ± 11b
10-30 kDa HA	-31.7±2.1a	115 ± 7b		-13.3±1.2c	221 ± 4c
3-10 kDa HA	-32.7±2.1a	119 ± 20b		-14.1±0.9d	312 ± 10d
< 3 kDa HA	-35.3±0.0a	118 ± 20b	33 ± 18	-18.6±0.4e	213 ± 10e
r*	0.062	0.902		0.723	0.341

Different lowercase letters in the same column indicate significant differences ($P < 0.05$) among different HA MW. *r is the correlation coefficient calculated by linear

regression analysis.

Table S3. Zeta potentials, particle size of QD-NH_2 in the absence and presence of pristine- and M_f-HA in 3 mM NaCl or 2 mM $CaCl_2$ solutions.

	NaCl			**$CaCl_2$**	
HA type	**Zeta potential (mV)**	**DLS diameter (nm)**	**TEM Diameter (nm)**	**Zeta potential (mV)**	**DLS diameter (nm)**
no HA	0.3±0.1	172 ± 13	32 ± 24	3.29±0.7	498 ± 24
pristine HA	-13.4±0.0	165 ± 33		-2.2±0.4	386 ± 2
>100 kDa HA	-11±0.9a	146 ± 17c	29 ± 22	-4.5±0.9a	312 ± 3a
30-100kDa HA	-10.4±0.7a	139 ± 12c		-3.8±0.1a	375 ± 2b
10-30 kDa HA	-7.0±0.3b	167 ± 19c		-2.5±0.3a	387 ± 13c
3-10 kDa HA	-14.8±0.2a	149 ± 5c		-4.9±0.3a	337 ± 22d
< 3 kDa HA	-19.9±1.3a	240 ± 7d	33 ± 18	-8.7±1.3b	400 ± 7e
r*	0.461	0.580		0.368	0.606

Different lowercase letters in the same column indicate significant differences ($P < 0.05$) among different HA MW. *r is the correlation coefficient calculated by linear

regression analysis.

Table S4. Mass Recoveries for Column Experiments.

Electrolyte	Particle	HA type	Recovery (%)		
			M_{eff}[a]	M_{ret}[b]	M_{tot}[c]
NaCl	QD-COOH	without HA	99.8 ± 0.9	0.5 ± 0.2	100.3 ± 1.1
		pristine HA	96.9 ± 1.4	2.2 ± 0.8	99.1 ± 0.8
		>100 kDa HA	99.6 ± 5.8	0.8 ± 5.0	100.4 ± 1.2
		30-100 kDa HA	97.0 ± 1.1	1.4 ± 1.5	98.4 ± 0.5
		10-30 kDa HA	97.8 ± 3.0	1.7 ± 3.9	99.5 ± 2.6
		3-10 kDa HA	97.1 ± 3.9	2.0 ± 4.2	99.6 ± 1.4
		< 3 kDa HA	97.5 ± 1.3	1.5 ± 0.6	99.0 ± 0.7
NaCl	QD-NH_2	without HA	0.3 ± 0.1	99.6 ± 0.2	99.9 ± 0.2
		pristine HA	86.9 ± 5.8	12.0 ± 5.0	98.9 ± 0.8
		>100 kDa HA	94.8 ± 0.2	5.5 ± 1.4	100.3 ± 1.2
		30-100 kDa HA	89.5 ± 1.5	10.0 ± 0.6	99.5 ± 2.1
		10-30 kDa HA	78.3 ± 0.7	20.6 ± 4.0	98.3 ± 4.7
		3-10 kDa HA	17.2 ± 9.4	68.4 ± 11.7	85.6 ± 2.3
		< 3 kDa HA	6.6 ± 0.5	90.6 ± 2.7	97.6 ± 2.2
$CaCl_2$	QD-COOH	without HA	0.0 ± 0.0	99.8 ± 0.1	99.8 ± 0.1
		pristine HA	2.8 ± 1.3	92.8 ± 1.5	95.6 ± 1.1
		>100 kDa HA	10.5 ± 0.3	83.5 ± 0.4	94.0 ± 0.3
		30-100 kDa HA	26.0 ± 1.7	75.2 ± 3.0	101.2 ± 1.3
		10-30 kDa HA	5.2 ± 0.5	91.1 ± 0.9	96.3 ± 0.4

		3-10 kDa HA	0. 4 ± 0.5	97.7 ± 2.7	98.1 ± 2.2
		< 3 kDa HA	2.6 ± 0.6	93.2 ± 1.3	95.8 ± 0.8
$CaCl_2$	$QD\text{-}NH_2$	without HA	0.0 ± 0.0	98.3 ± 1.3	98.3 ± 1.3
		pristine HA	2.6 ± 0.6	92.5 ± 0.4	95.1 ± 1.0
		>100 kDa HA	0.1 ± 1.7	94.4 ± 3.0	94.5 ± 3.0
		30-100 kDa HA	0.0 ± 0.0	97.3 ± 1.1	97.3 ± 1.1
		10-30 kDa HA	0.0 ± 0.0	101.9 ± 0.1	101.9 ± 0.1
		3-10 kDa HA	0.0 ± 0.0	97.1 ± 5.4	97.1 ± 5.4
		< 3 kDa HA	6.3 ± 0.5	90.6 ± 2.7	96.9 ± 0.1

[a]M_{eff}, [b]M_{ret} and [c]M_{tot} refer to the effluent, retained, and total percentages of QDs recovered from column experiments, respectively. All values represent the relative percentage of the QDs particles by mass. M_{eff} was determined by integrating beneath the effluent concentration profiles in Figure 3a,b, Figure 4a,b, Figure 5a,b and Figure 6a,b. M_{ret} was determined by the retention progiles in Figure 3c,d, Figure 4c,d, Figure 5c,d and Figure 6c,d.

Table S5. The adsorbed amount of HA on the QDs surface and calculated adsorbed layer thickness of HA in the presence of pristine- and M_f-HA under different electrolytes.

Electrolyte	**Particle**	**HA type**	**The adsorption amount of HA (mg/m^2)**	**Adsorbed layer thickness (nm)**
NaCl	QD-COOH	no HA	/	/
		pristine HA	0.602 ± 0.0140	5.65
		>100 kDa HA	0.902 ± 0.0007	5.80
		30-100 kDa	0.662 ± 0.0028	5.63
		10-30 kDa HA	0.614 ± 0.0021	5.62
		3-10 kDa HA	0.566 ± 0.0057	5.60
		< 3 kDa HA	0.422 ± 0.0035	5.60
NaCl	$QD\text{-}NH_2$	no HA	/	/
		pristine HA	0.630 ± 0.0064	7.30
		>100 kDa HA	1.777 ± 0.0011	7.90
		30-100 kDa	1.777 ± 0.0074	8.00
		10-30 kDa HA	1.347 ± 0.0034	6.92
		3-10 kDa HA	0.644 ± 0.0007	6.85
		< 3 kDa HA	0.640 ± 0.0007	6.83
		no HA	/	/
		pristine HA	2.088 ± 0.0085	5.86
		>100 kDa HA	2.525 ± 0.0028	6.60

		30-100 kDa	2.389 ± 0.0035	6.40
		10-30 kDa HA	1.385 ± 0.0120	5.90
		3-10 kDa HA	1.206 ± 0.0000	5.65
		< 3 kDa HA	0.630 ± 0.0064	5.60
$CaCl_2$	$QD\text{-}NH_2$	no HA	/	/
		pristine HA	2.159 ± 0.0000	7.90
		>100 kDa HA	2.882 ± 0.0021	8.30
		30-100 kDa	2.882 ± 0.0021	8.20
		10-30 kDa HA	1.514 ± 0.0049	7.40
		3-10 kDa HA	1.228 ± 0.0591	7.10
		< 3 kDa HA	1.127 ± 0.0028	6.90

Table S6. Zeta potentials of sand in mono- and divalent electrolyte with or without pristine- and M_f-HA.

Electrolyte	HA type	Zeta potential (mV)
NaCl	without HA	-43.8 ± 1.1
	pristine HA	-46.6 ± 0.4
	>100 kDa HA	-41.1 ± 1.5
	30-100 kDa HA	-50.8 ± 1.9
	10-30 kDa HA	-35 ± 1.5
	3-10 kDa HA	-43.6 ± 0.7
	< 3 kDa HA	-40.7 ± 1.5
$CaCl_2$	without HA	-21.5 ± 1.2
	pristine HA	-19.2 ± 1.3
	>100 kDa HA	-17.3 ± 0.7
	30-100 kDa HA	-19.5 ± 1.2
	10-30 kDa HA	-16 ± 1.6
	3-10 kDa HA	-14.7 ± 2.5
	< 3 kDa HA	-16.0 ± 2.4

Supplemental Figures:

Figure S1. Calculated DLVO interaction energy profiles between QDs and sand in NaCl (a) and $CaCl_2$ (b) electrolytes without HA.

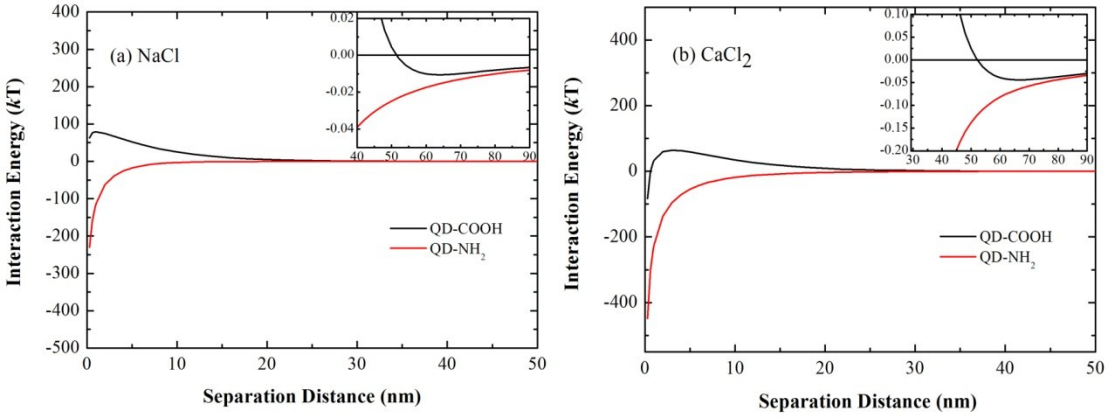

Figure S2. Calculated modified DLVO interaction energy profiles between QD-COOH and sand in NaCl electrolytes with 5mg/L pristine- and M_f-HA.

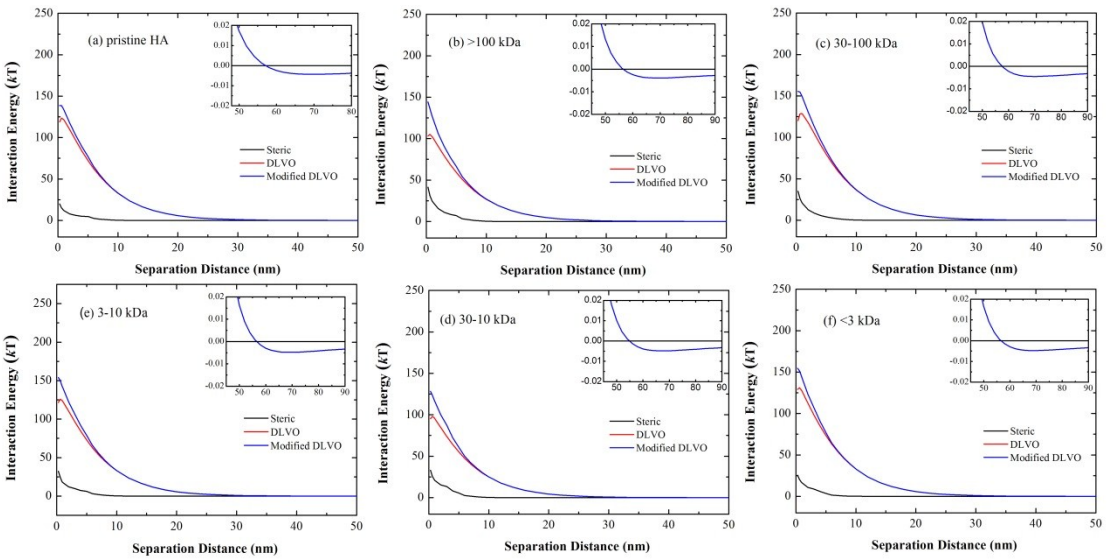

Figure S3. Calculated modified DLVO interaction energy profiles between QD-NH_2 and sand in NaCl electrolytes with 5mg/L pristine- and M_f-HA.

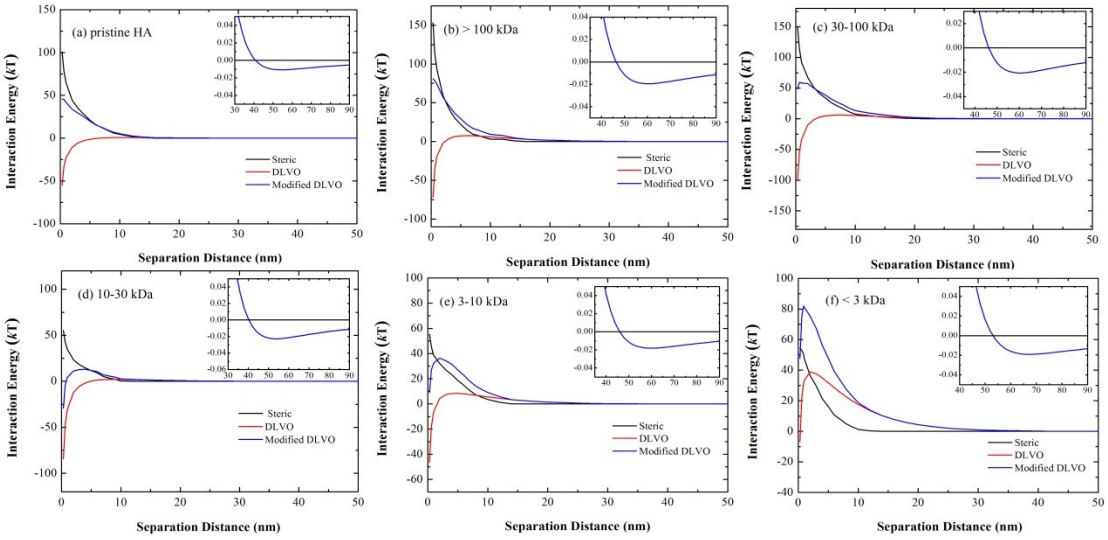

Figure S4. Calculated modified DLVO interaction energy profiles between QD-COOH and sand in $CaCl_2$ electrolytes with 5mg/L pristine- and M_f-HA.

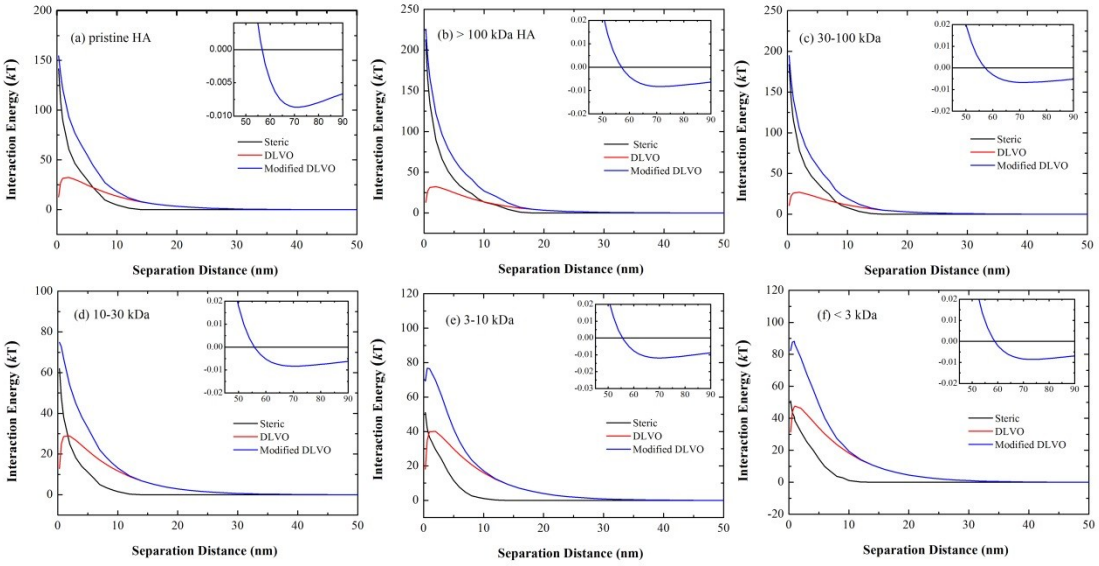

Figure S5. Calculated modified DLVO interaction energy profiles between QD-NH_2 and sand in $CaCl_2$ electrolytes with 5mg/L pristine- and M_f-HA.

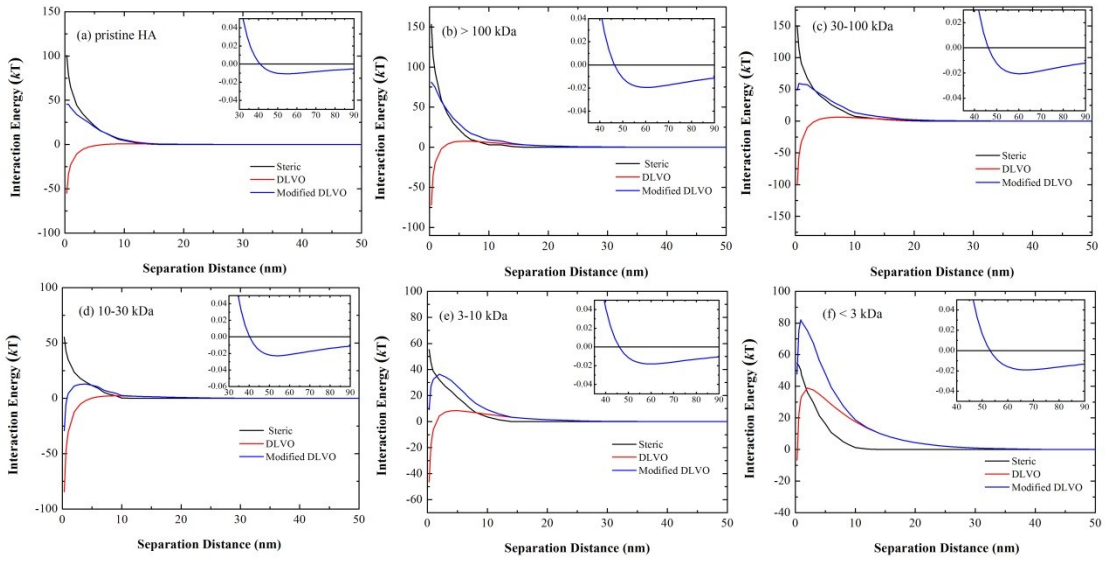

Figure S6. SEM image of quartz sand surface.

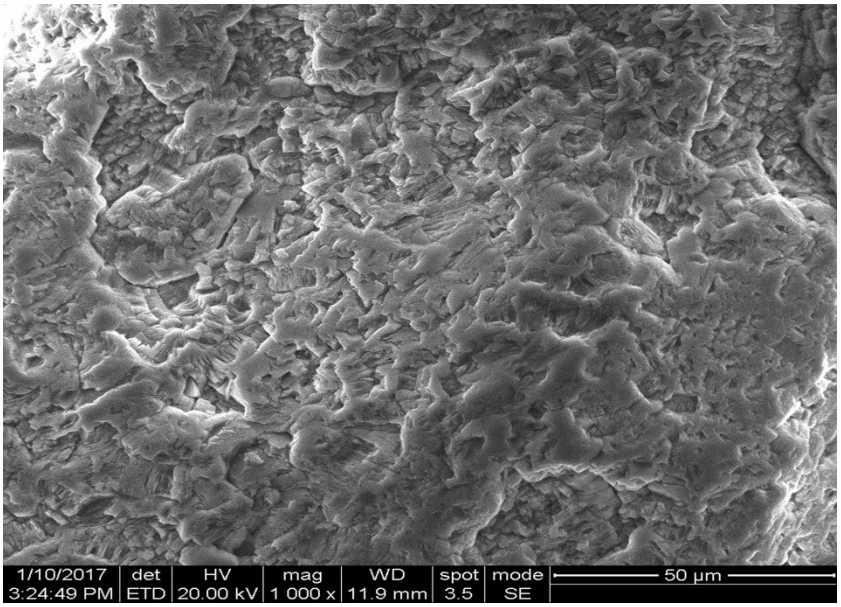

Reference

1. I. R. Quevedo and N. Tufenkji, *Environ. Sci. Technol.*, 2012, **46**, 4449-4457.
2. S. Torkzaban, Y. Kim, M. Mulvihill, J. Wan and T. K. Tokunaga, *J. Contam. Hydrol.*, 2010, **118**, 208-217.
3. S. Torkzaban, S. A. Bradford, J. Wan, T. Tokunaga and A. Masoudih, *Environ. Sci. Technol.*, 2013, **47**, 11528-11536.
4. A. C. Maizel and C. K. Remucal, *Environ. Sci. Technol.*, 2017, **51**, 2113-2123.
5. M. H. Shen, Y. G. Yin, A. Booth and J. F. Liu, *Water Res.*, 2015, **71**, 11-20.
6. V. L. Morales, W. Zhang, B. Gao, L. W. Lion, J. J. Bisogni, Jr., B. A. McDonough and T. S. Steenhuis, *Water Res.*, 2011, **45**, 1691-1701.
7. T. Phenrat, J. E. Song, C. M. Cisneros, D. P. Schoenfelder, R. D. Tilton and G. V. Lowry, *Environ. Sci. Technol.*, 2010, **44**, 4531-4538.
8. H. Ohshima, *Advan. Colloid Interface Sci.*, 1995, **62**, 189-235.

9. H. Ohshima, M. Nakamura and T. Kondo, *Colloid Polymer Sci.*, 1992, **270**, 873-877.

10. G. Zeng, J. Wan, D. Huang, L. Hu, C. Huang, M. Cheng, W. Xue, X. Gong, R. Wang and D. Jiang, *J. Hazard Mater*, 2017, **339**, 354-367.

11. C. Lai, M.-M. Wang, G.-M. Zeng, Y.-G. Liu, D.-L. Huang, C. Zhang, R.-Z. Wang, P. Xu, M. Cheng, C. Huang, H.-P. Wu and L. Qin, *Appl. Surf. Sci.*, 2016, **390**, 368-376.

12. C. J. V. Oss, *J.Mol. Recogn.*, 2003, **16**, 177-190.

13. B. Chu, *Intermolecular and Surface Forces with Applications to Colloidal and Biological Systems. by Jacob N. Israelachvili*, Academic Press1985.

14. E. Rabani, *J. Chemi. Physics*, 2002, **116**, 258-262.

15. J. D. Hu, Y. Zevi, X. M. Kou, J. Xiao, X. J. Wang and Y. Jin, *Sci. Total Environ.*, 2010, **408**, 3477-3489.

16. X. Lv, B. Gao, Y. Y. Sun, X. Q. Shi, H. X. Xu and J. C. Wu, *Water Air Soil Pollut*., **2014**, 216-225.

17. T. Phenrat, N. Saleh, K. Sirk, H. J. Kim, R. D. Tilton and G. V. Lowry, *J. Nanoparticle Res.*, 2008, 10: 795-814.